

Tracking Control of Time-Varying Discontinuous Trajectories with Application to Probe-Based Imaging and Nanopositioning

Saeid Bashash, Reza Saeidpourazar, and Nader Jalili

Abstract— In this effort, a supervisory switching control strategy is proposed for effective control of piezoelectric actuators in tracking harmonic trajectories with sudden discontinuities. A piezoelectrically-driven nanopositioning stage with high resolution capacitive position sensor is utilized in a set of experiments to study the performance of controllers tuned for tracking of continuous trajectories in tracking of stepped trajectories, and vice versa. Using a mixed Lyapunov-based robust adaptive and PID controller, it is observed that the controllers tuned for continuous trajectory tracking demonstrate large oscillations with light damping rate in tracking of stepped inputs. Conversely, when they are tuned for smoother step tracking, poor performance is achieved in tracking of continuous trajectories within a desired frequency range. Hence, a switching strategy is proposed to track desired trajectories using two controllers separately tuned for continuous and stepped trajectories. Switching conditions and transformation laws are then derived and experimentally implemented. Results indicate that the proposed framework presents higher performance compared to the individual controllers in tracking of discontinuous trajectories.

I. INTRODUCTION

A variety of current technological applications utilize piezoelectric positioning devices to generate controlled motions with fast positioning accuracies. Particularly, piezoelectric devices have been extensively utilized in optics [1], medical surgery [2], microfabrication [3], metrology [4], and many other applications with enabling ultra-accurate operations. Scanning Probe Microscopy (SPM) is a widely used application for atomic and molecular level imaging of materials' surfaces and manipulation of nano-size objects [5-7]. In a typical SPM, the task of the probe attached to a positioning stage is to scan and track the surface of samples with random topography variations. Thus, precision and robustness are key factors for achieving high-performance control through piezoelectric systems.

Tracking control of piezoelectric devices is limited by a number of structural and dynamical effects. Hysteresis

phenomenon with its multiple-loop behavior is the most limiting factor in accurate positioning of piezoelectric systems. All feedforward control strategies need an inverse model to compensate the hysteresis effect [8-10]. However, there are different scenarios in the closed-loop control. Although many feedback strategies have utilized hysteresis model as an essential part of their controller [11-13], a few have precisely controlled their plant without including a hysteresis model [14, 15]. The latter methods utilize robust control schemes instead, relying on the fact that hysteresis represents a bounded disturbance [15]. Hence, the controller can suppress hysteresis effect if it is made robust enough.

System dynamics are also important in tracking problem, especially when precision in a broad frequency range is desired. The dynamics of piezoelectric systems are described by distributed-parameters representation expressed by partial differential equations [16]. However, depending on the frequency of operation, the system can be safely reduced to lumped-parameters representation. Although a few references have adopted distributed-parameters models [16, 17], many others have considered lumped-parameters representation [12-14]. Their justification relies on the fact that piezoelectric stages usually have higher resonant frequencies than the operational frequency. Hence, the need for modeling of higher modes is eliminated when operating below the first resonance.

System constant parameters contain uncertainties due to the identification inaccuracy, and are subjected to change because of aging and the environmental variations. Hence, the collective parametric errors can induce disturbance-like forces and degrade the control performance. This necessitates the need to augment the controller to adaptive laws for such system unknown parameters [14, 15]. The incorporation of the robust and adaptive features into the control design would lead to high-performance tracking of desired trajectories in a broad frequency range despite the unmodeled hysteresis effect and parametric uncertainties.

In general, controllers designed for tracking of time-varying trajectories are tuned for continuously differentiable trajectories. Hence, discontinuities in the desired trajectory may lead to significant oscillations of the closed-loop system. In many applications, the desired trajectory is not stipulated, and may change suddenly in real-time. Hence, the controller must be prepared for such events.

In this article, a switching controller is proposed for effective tracking control of high-frequency trajectories with discontinuities. The controller structure is based on

Manuscript received September 19, 2008. The materials presented here are based upon work supported by the National Science Foundation under CAREER Grant No. CMMI-0238987. Any opinions, findings, and conclusions or recommendations expressed in this material are those of the authors and do not necessarily reflect the views of the National Science Foundation.

Authors are with the Smart Structures and Nanoelectromechanical Systems Laboratory, Department of Mechanical Engineering, Clemson University, Clemson, SC 29634-0921 (N. Jalili is associate professor and the corresponding author, phone: 864-656-5642; fax: 864-656-4435; e-mail: jalili@clemson.edu).

switching between two separate control modes: a Lyapunov-based robust adaptive tracking controller and a PID step controller. The proposed strategy is shown to offer excellent performance in tracking of high-frequency trajectories with discontinuities. This strategy is expected to be effectively implemented in SPMs for nano-manipulation and imaging applications.

II. MODELING AND CONTROL OF PIEZOELECTRIC SYSTEMS

To effectively track a time-varying continuous trajectory in practice, the controller must be made robust with respect to the ever-present disturbances and uncertainties in system parameters. In this section, a Lyapunov-based robust adaptive control law derived in [14] is utilized for precision tracking control of the system. This controller has been shown to possess a good performance despite the parametric uncertainties and unmodeled hysteresis effect.

A. System Modeling

A widely-used model for piezoelectric positioning systems is a linear second order dynamics with hysteretic excitation given by [12-14]:

$$\ddot{x}(t) + 2\zeta\omega_n\dot{x}(t) + \omega_n^2x(t) = \omega_n^2H\{v(t)\} \quad (1)$$

where $x(t)$ and $v(t)$ stand for the system displacement and applied input voltage, respectively, ζ and ω_n are the system damping ration and natural frequency, respectively, and $H\{v(t)\}$ represents a scaled hysteretic relation between the applied voltage and the generated force through the piezoelectric stack. It is well known that hysteresis is a bounded phenomenon [15] which can be divided into a linear segment and a bounded variation as:

$$H\{v(t)\} = a(v(t) + v_h(t)), \quad |v_h(t)| \leq M \quad (2)$$

where a is the average slope of hysteresis and M is the finite bound of its variation from the linear approximation. Hence, Eq. (1) can be recast as:

$$m\ddot{x}(t) + c\dot{x}(t) + kx(t) = v(t) + v_h(t) \quad (3)$$

$$m = \frac{1}{a\omega_n^2}, \quad c = \frac{2\zeta}{a\omega_n}, \quad k = \frac{1}{a}, \quad r = \frac{b}{a}$$

Considering the collective effects of $v_h(t)$ and the ever-present external and internal disturbances as a single bounded input with a static and a dynamic portion leads to:

$$m\ddot{x}(t) + c\dot{x}(t) + kx(t) = v(t) + (d_c + d(t)), \quad |d(t)| \leq N \quad (4)$$

with d_c and $d(t)$ being the respective constant (static) and dynamic disturbances, and N being a finite value representing the bound of the dynamic disturbance.

B. Robust Adaptive Control

In [14], a globally uniformly ultimately bounded Lyapunov-based controller has been developed for robust adaptive tracking control of piezoelectric systems with their essential dynamics described by Eq. (4). Defining the

tracking error as $e(t) = x_d(t) - x(t)$ with $x_d(t)$ being the desired trajectory, the proposed control law is given by:

$$v(t) = \hat{m}(t)(\ddot{x}_d(t) + \sigma\dot{e}(t)) + \hat{c}(t)\dot{x}(t) + \hat{k}(t)x(t) - \hat{d}_c(t) + \eta_1s(t) + \eta_2\text{sat}(s(t)/\varepsilon) \quad (5)$$

where σ , η_1 , η_2 and ε are positive control parameters satisfying $N < \eta_2$, $s(t) = \dot{e}(t) + \sigma e(t)$,

$$\begin{aligned} \hat{m}(t) &= \hat{m}(0) + \frac{1}{k_1} \int_0^t \text{Proj}_m [s(\tau)(\ddot{x}_d(\tau) + \sigma\dot{e}(\tau))] d\tau \\ \hat{c}(t) &= \hat{c}(0) + \frac{1}{k_2} \int_0^t \text{Proj}_c [s(\tau)\dot{x}(\tau)] d\tau \\ \hat{k}(t) &= \hat{k}(0) + \frac{1}{k_3} \int_0^t \text{Proj}_k [s(\tau)x(\tau)] d\tau \\ \hat{d}_c(t) &= \hat{d}_c(0) + \frac{1}{k_4} \int_0^t \text{Proj}_{d_c} [-s(\tau)] d\tau \end{aligned} \quad (6)$$

are the adaptation laws with k_1 to k_4 being adaptation gains, $\hat{m}(0)$ to $\hat{d}_c(0)$ being approximate parameter values with known lower and upper bounds, and $\text{Proj}_\theta[X]$ is the projection operator given by:

$$\text{Proj}_\theta[X] = \begin{cases} 0 & \text{if } \hat{\theta}(t) = \theta_{\max} \text{ and } X > 0 \\ 0 & \text{if } \hat{\theta}(t) = \theta_{\min} \text{ and } X < 0 \\ X & \text{otherwise} \end{cases} \quad (7)$$

where $\hat{\theta}(t)$ represents the adaptation variable (e.g., $\hat{m}(t)$, $\hat{c}(t)$, etc.) with θ_{\min} and θ_{\max} being its lower and upper bounds, respectively. The utilization of projection operator guarantees that all the adaption variables stay bounded by their lower and upper values, while the stability of closed-loop system is enhanced. Moreover, the saturation term in Eq. (5) is associated with the robustness feature of controller against the dynamic disturbances including the hysteresis variations. Based on a Lyapunov analysis, the bound of steady-state error amplitude can be explicitly expressed as a function of control gains as follows:

$$|e_{ss}(t)| \leq \frac{\eta_2\varepsilon}{\sigma(\eta_1\varepsilon + \eta_2)} \quad (8)$$

The full proof of the proposed control law is given in [14], and is omitted here for the sake of brevity. However, several experiments are performed here to show the effectiveness of the proposed method compared to the PID controller in tracking control of piezoelectrically-driven systems.

C. Experimental Control Results

A Physik Instrumente P-753.11c PZT-driven nanopositioning stage as shown in Fig. 1 is used for the experiments here. Experimental data interfacing is carried out through a Physik Instrumente E-500 chassis for actuator amplifier and position servo-controller along with dSPACE® data acquisition (DS1103) controller board. The

sampling rate of the controller is set to 20 kHz, and the position of the stage is measured by a sub-nanometer resolution built-in capacitive sensor.

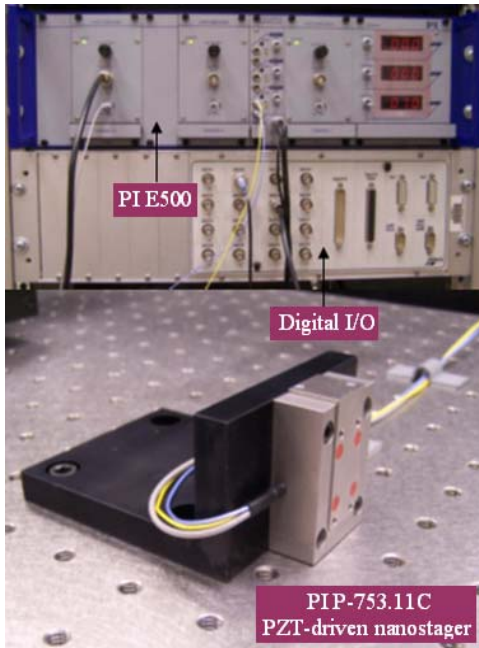


Fig. 1. Experimental setup for the PZT-driven nano-positioning stage.

To verify the effectiveness of the proposed robust adaptive control law in a broad frequency range, a $1\ \mu\text{m}$ amplitude desired chirp trajectory is considered with linear frequency increase from 0 to 300 Hz within 30 seconds. To comparatively assess the effectiveness of the proposed control law, a PID controller is implemented as well. The gains of both controllers are tuned in such a way that they operate near their best performance for the applied input.

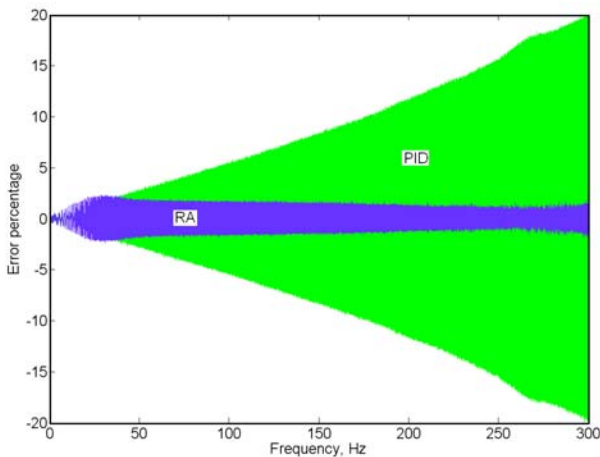


Fig. 2. Tracking error comparison between well-tuned robust adaptive and PID controllers for a $1\ \mu\text{m}$ amplitude chirp trajectory from 0 to 300 Hz.

Fig. 2 depicts the chirp tracking results. As seen, the proposed robust adaptive controller maintains a good level of performance for the entire frequency range, especially for higher frequencies. There is a 2.5% peak for maximum

tracking error at about 25 Hz, while for most of the frequencies this value stays below 2%. The PID controller produces a linear increase in error amplitude with respect to frequency. Although it presents better performance compared to the robust adaptive controller initially, its performance starts to degrade after about 30 Hz. Tracking with PID controller can lead to 20% maximum error percentage at 300 Hz, indicating that it is less effective than robust adaptive controller in high frequencies.

Since many applications require tracking of step-like trajectories, a 50 Hz rectangular reference signal is applied to assess the performance of these controllers. Fig. 3 depicts the system response using PID and robust adaptive controllers. Although both controllers offer stable convergence to the desired trajectory, their transient response includes undesirable large oscillations. Hence, the control gains are re-tuned to present better and faster transient response for stepped trajectory as shown in Fig. 4. However, when these gains are utilized for tracking of previous chirp trajectory, they yield lower tracking performance. This has been shown in Fig. 5, where the robust adaptive controller presents about 7% maximum error around 40 Hz while the PID controller yields about 75% error at 300 Hz.

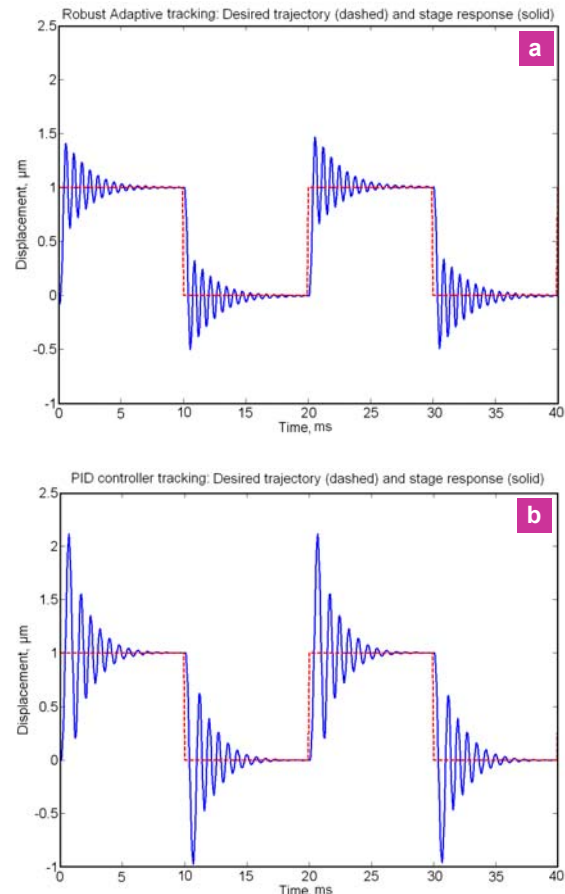


Fig. 3. Stepped trajectory tracking using (a) robust adaptive and (b) PID controllers tuned for *chirp* tracking.

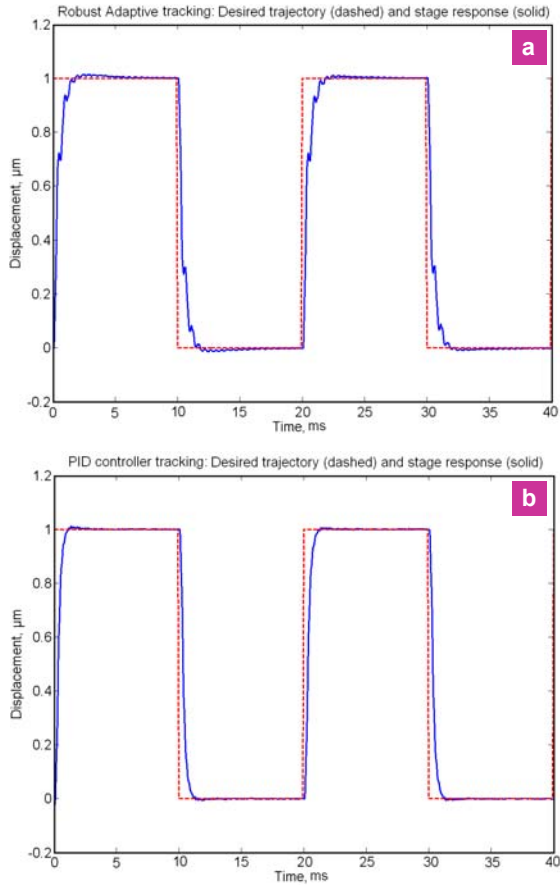


Fig. 4. Stepped trajectory tracking using (a) robust adaptive and (b) PID controllers tuned for *step* tracking.

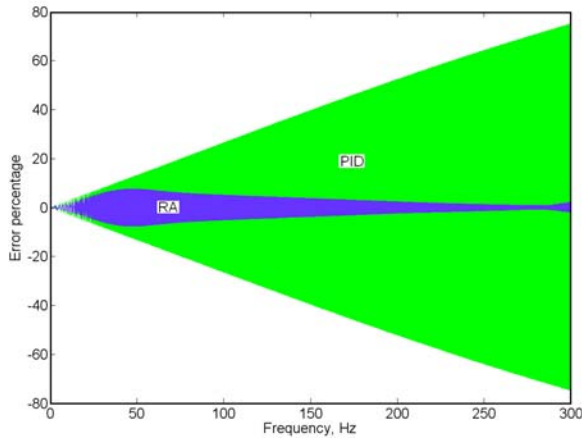


Fig. 5. Tracking results of $1 \mu\text{m}$ amplitude chirp trajectory from 0 to 300 Hz for robust adaptive and PID controllers tuned for *step* tracking.

In SPM applications, the piezoelectric stage is responsible for tracking surface topographies with multiple-frequency components and frequent stepped-like discontinuities. Choosing robust adaptive controller for tracking continuous trajectories and PID controller for tracking stepped trajectories, two experiments are carried out here for tracking of a representative harmonic trajectory with stepped discontinuities. Fig. 6 validates that both robust adaptive and PID controllers, when implemented individually, cannot present acceptable results for such trajectories.

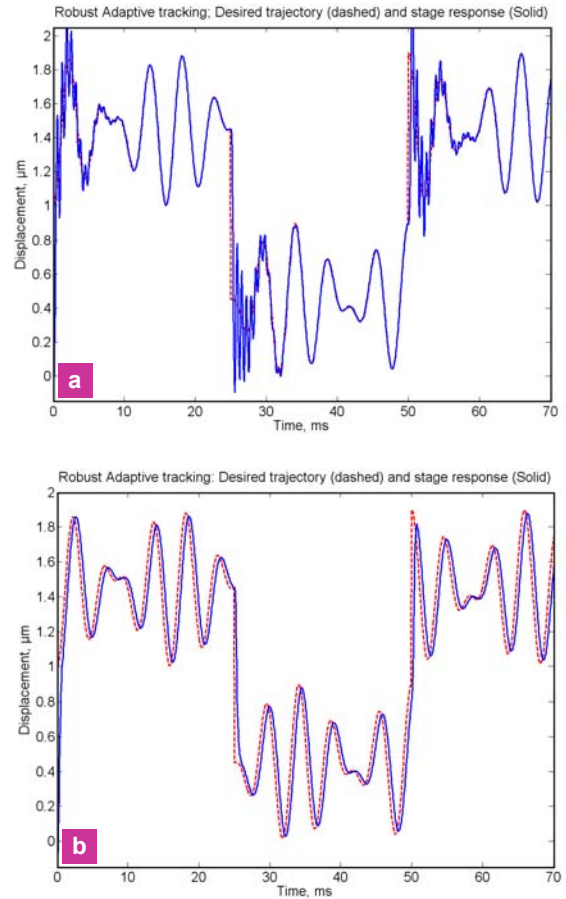


Fig. 6. Tracking multiple-frequency discontinuous trajectory: (a) Robust adaptive controller tuned for *chirp* tracking, and (b) PID controller tuned for *step* tracking.

III. SWITCHING CONTROLLER DESIGN

The objective of switching control is to systematically assign different controllers to the system to achieve desired objectives with conflicting requirements. More specifically, we intend to use the robust adaptive controller for tracking of continuous trajectories and switch to PID controller in the event of trajectory jumps. Hence, two switching conditions need to be specified: (i) the condition for switching to PID controller, and (ii) condition for switching back to the robust adaptive controller.

When a jump occurs in the desired trajectory, the position error $e(t)$ changes suddenly, depending on the jump amplitude; however, the time derivative of the position error $\dot{e}(t)$ which is approximated by $(e(t) - e(t - \Delta t)) / \Delta t$ grows significantly at the jump instant because of sudden error change in a small time step Δt . Hence, it can be a good indicator of discontinuity in the desired trajectory for switching to PID controller. That is, when $\dot{e}(t)$ becomes greater than a preset threshold, i.e. $|\dot{e}(t)| > e_{thr}$, and the robust adaptive controller is in charge of tracking, the supervisory control law must switch to PID controller and wait until system response converges to the desired trajectory. Once the position error $e(t)$ reaches near zero, i.e.

$|e(t)| < e_{rr}$, while the PID controller is operating, the supervisory control law must switch to the robust adaptive controller again to achieve the ideal performance in tracking of the desired trajectory. The proposed switching control law can be formulated as:

$$v(t) = \begin{cases} v_{PID}(t) : & (\text{if } v(t-\Delta t) \in \text{PID} \ \& \ |e(t)| > e_{rr}) \text{ or} \\ & (\text{if } v(t-\Delta t) \in \text{RA} \ \& \ |\dot{e}(t)| > e_{dtr}) \\ v_{RA}(t) : & (\text{if } v(t-\Delta t) \in \text{PID} \ \& \ |e(t)| \leq e_{rr}) \text{ or} \\ & (\text{if } v(t-\Delta t) \in \text{RA} \ \& \ |\dot{e}(t)| \leq e_{dtr}) \end{cases} \quad (9)$$

where the term $v(t-\Delta t) \in X$ means the control input at the previous time step is generated by controller X . Eq. (9) states that the control strategy must stay the same or switch to another strategy if one of the switching conditions holds true.

Switching stability and performance depends on a number of matching conditions at the switching moments. Particularly, when a switching occurs, the activated controller starts a new task. Hence, a transformation is needed for the time and position coordinates. Fig. 7 demonstrates switching between the two controllers. At every switching moment, the time and position are set to zero for the new control task, meaning the coordinates are transformed to the switching position.

Denoting the i^{th} switching time as t_{si} , and constructing the i^{th} coordinate system based on t_i and $x_i(t_i)$, the following transformations can be given:

$$\begin{aligned} t_i &= t - t_{si}, \quad t_{si} < t \\ x_i(t_i) &= x(t) - x(t_{si}) \\ x_{di}(t_i) &= x_d(t) - x(t_{si}) \end{aligned} \quad (10)$$

which results in:

$$\begin{aligned} \dot{x}_i(t_i) &= \dot{x}(t) - \dot{x}(t_{si}) = \dot{x}(t) \\ \dot{x}_{di}(t_i) &= \dot{x}_d(t) - \dot{x}(t_{si}) = \dot{x}_d(t) \Rightarrow \ddot{x}_{di}(t_i) = \ddot{x}_d(t) \\ e_i(t_i) &= x_{di}(t_i) - x_i(t_i) = e(t) \Rightarrow \dot{e}_i(t_i) = \dot{e}(t) \\ s_i(t_i) &= \dot{e}_i(t_i) + \sigma e_i(t_i) = \dot{e}(t) + \sigma e(t) = s(t) \end{aligned} \quad (11)$$

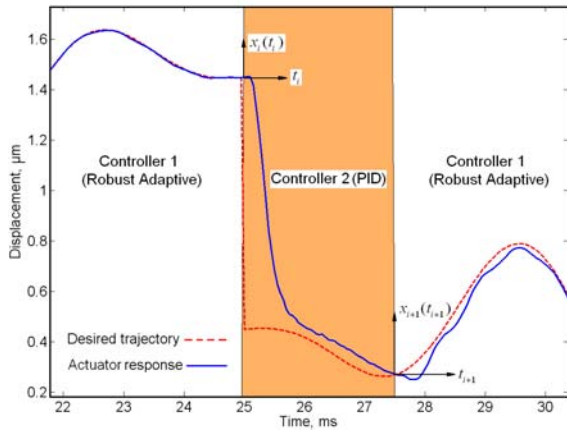


Fig. 7. A typical step tracking within tracking of a continuous trajectory (controller switches from robust adaptive to PID at the step instant and then switches back to the robust adaptive strategy when the response converges).

Moreover, the adaptation and PID integrals after the switching instance are reset due to the time transformation. For a general function $f_i(t_i)$, this can be written as:

$$\int_0^{t_i} f_i(\tau) d\tau = \int_{t_{si}}^t f(\tau) d\tau \quad (12)$$

Since the coordinates are transformed, the control input must be transformed as well. That is:

$$v_i(t_i) = v(t) - v(t_{si}), \quad t_{si} < t \quad (13)$$

Considering the transformation proposed by Eq. (10) and the results of Eqs. (11) and (12), if the i^{th} switching is from robust adaptive controller to PID controller, we can write:

$$\begin{aligned} v_{PID}(t) &= v(t_{si}) + v_i(t_i) = v(t_{si}) + k_p e(t) + \\ & k_I \int_{t_{si}}^t e(\tau) d\tau + k_D \dot{e}(t), \quad t_{si} < t \end{aligned} \quad (14)$$

And, if the i^{th} switching is from PID controller to robust adaptive controller, we have:

$$\begin{aligned} v_{RA}(t) &= v(t_{si}) + v_i(t_i) \\ &= v(t_{si}) + \hat{m}_i(t_i) (\ddot{x}_d(t) + \sigma \dot{e}(t)) + \hat{c}_i(t_i) \dot{x}(t) + \\ & \hat{k}_i(t_i) (x(t) - x(t_{si})) - \hat{d}_{ci}(t_i) + \eta_1 s(t) + \\ & \eta_2 \text{sat}(s(t) / \varepsilon), \quad t_{si} < t \end{aligned} \quad (15)$$

where

$$\begin{aligned} \hat{m}_i(t_i) &= \hat{m}(0) + \frac{1}{k_1} \int_{t_{si}}^t \text{Proj}_{m_i} [s(\tau) (\ddot{x}_d(\tau) + \sigma \dot{e}(\tau))] d\tau \\ \hat{c}_i(t_i) &= \hat{c}(0) + \frac{1}{k_2} \int_{t_{si}}^t \text{Proj}_{c_i} [s(\tau) \dot{x}(\tau)] d\tau \\ \hat{k}_i(t_i) &= \hat{k}(0) + \frac{1}{k_3} \int_{t_{si}}^t \text{Proj}_{k_i} [s(\tau) (x(\tau) - x(t_{si}))] d\tau \\ \hat{d}_{ci}(t_i) &= \hat{d}_c(0) + \frac{1}{k_4} \int_{t_{si}}^t \text{Proj}_{d_{ci}} [-s(\tau)] d\tau \end{aligned} \quad (16)$$

Eqs. (14)-(16) represent the final forms of control laws for the proposed switching strategy. It is remarked that only three changes are made in the control inputs and their corresponding signals: (i) resetting the integrals, (ii) recording the control input at the switching instance $v(t_{si})$ and adding it to the original control input after switching, and (iii) transforming the position feedback $x(t)$ to $x(t) - x(t_{si})$.

Fig. 8 demonstrates a flowchart of the proposed switching control strategy. Setting the initial controller to robust adaptive, the condition for stepped trajectory is checked; if the answer is positive, the controller switches to PID, and if it is negative, it stays on the robust adaptive strategy until a step occurs. If the strategy is on PID, the controller checks whether the actuator response has reached the desired trajectory or not; if the answer is positive, it switches back to robust adaptive, otherwise it stays on PID. The controller keeps tracking until a termination command is applied. It is remarked that any control pairs, one tuned for step tracking and the other tuned for continuous trajectory tracking can be implemented using the proposed switching strategy.

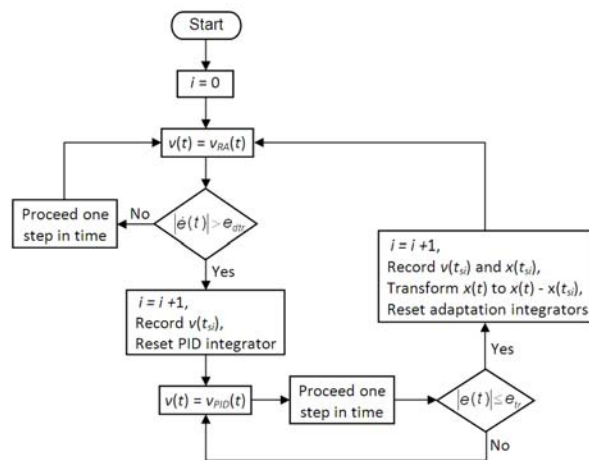


Fig. 8. Flowchart of the proposed switching strategy between robust adaptive and PID controllers.

The multiple-frequency sinusoidal trajectory depicted in Fig. 6 is given to the switching controller to assess its tracking performance. The switching thresholds are set to $e_{dr} = 5 \times 10^{-4} \text{ m/sec}$ (corresponding to 25 nm step in $5 \times 10^{-5} \text{ sec}$ time interval) and $e_r = 5 \text{ nm}$. Fig. 9 depicts the tracking results. As seen, the designed switching controller is able to smoothly track a trajectory of combined jumps and high-frequency sinusoids with excellent performance compared to the results depicted in Fig. 6.

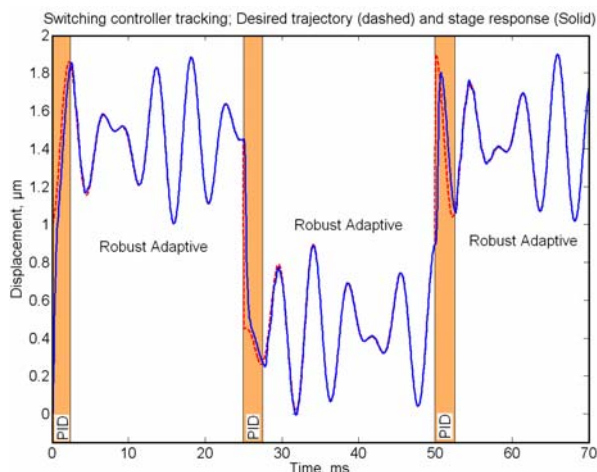


Fig. 9. Tracking multiple-frequency harmonic trajectory with discontinuities using the proposed switching control strategy.

IV. CONCLUSIONS

A switching control strategy was proposed for effective control of piezoelectric actuators in tracking discontinuous trajectories. A Lyapunov-based robust adaptive controller and a PID controller were utilized to study their performance in tracking of chirp and stepped trajectories. It was shown that when the controllers were tuned for chirp tracking, they induced large oscillations for stepped trajectories. Conversely, when they were tuned for step tracking, they demonstrated low-performance chirp tracking. Moreover, the robust adaptive controller offered more

effective performance than PID in chirp tracking, but less for tracking of stepped trajectories. Hence, a switching strategy was proposed to decide between the robust adaptive and PID controllers tuned for chirp and step tracking, respectively. The proposed strategy was implemented experimentally, and resulted in significant improvements using the proposed controller compared to the individual controllers.

REFERENCES

- [1] S. Aoshima, N. Yoshizawa, and T. Yabuta, "Compact mass axis alignment device with piezo elements for optical fibers," *IEEE Photonics Technology Letters*, vol. 4, pp. 462-464, 1992.
- [2] H. Akahori, Y. Haga, T. Matsunaga, K. Totsu, H. Iseki, M. Esashi, and H. Wada, "Piezoelectric 2D microscanner for precise laser treatment in the human body," *3rd IEEE/EMBS Special Topic Conference on Microtechnology in Medicine and Biology*, pp. 166 - 169, Oahu, Hawaii, May 2005.
- [3] J. Hesselbach, R. Ritter, R. Thoben, C. Reich, and G. Pokar, "Visual control and calibration of parallel robots for micro assembly," *Proceedings of SPIE*, vol. 3519, pp. 50-61, Boston, MA, Nov. 1998.
- [4] H. Haitjema, "Dynamic probe calibration in the μm region with nanometer accuracy," *Precision Engineering*, vol. 19, pp. 98-104, 1996.
- [5] G. Binnig, and H. Rohrer, "Surface imaging by scanning tunneling microscopy," *Ultramicroscopy*, vol. 11, pp. 157-160, 1983.
- [6] S. Gonda, T. Doi, T. Kurosawa, Y. Tanimura, N. Hisata, T. Yamagishi, H. Fujimoto, and H. Yukawa, "Accurate topographic images using a measuring atomic force microscope," *Applied Surface Science*, vol. 144-145, pp. 505-509, 1999.
- [7] R. Curtis, T. Mitsui, and E. Ganz, "Ultrahigh vacuum high speed scanning tunneling microscope," *Review of Scientific Instruments*, vol. 68, pp. 2790-2796, 1997.
- [8] S. Bashash and N. Jalili, "Intelligent rules of hysteresis in feedforward trajectory control of piezoelectrically-driven nanostagers," *Journal of Micromechanics and Microengineering*, vol. 17, pp. 342-349, 2007.
- [9] K. Kuhnen and H. Janocha, "Inverse feedforward controller for complex hysteretic nonlinearities in smart-material systems," *Control and Intelligent System*, vol. 29, pp. 74-83, 2001.
- [10] S. Lining, R. Changhai, R. Weibin, C. Ligu, and K. Minxiu, "Tracking control of piezoelectric actuator based on a new mathematical model," *Journal of Micromechanics and Microengineering*, vol. 14, pp. 1439-1444, 2004.
- [11] G. Tao and P. V. Kokotovic, "Adaptive control of plants with unknown hysteresis," *IEEE Transactions on Automatic Control*, vol. 40, pp. 200-212, 1995.
- [12] J. J. Tzen, S. L. Jeng, and W. H. Chieng, "Modeling of piezoelectric actuator for compensation and controller design," *Precision Engineering*, vol. 27, pp. 70-76, 2003.
- [13] S. Bashash and N. Jalili, "Robust multiple-frequency trajectory tracking control of piezoelectrically-driven micro/nano positioning systems," *IEEE Transactions on Control Systems Technology*, vol. 15, pp. 867-878, 2007.
- [14] S. Bashash and N. Jalili, "Robust adaptive control of coupled parallel piezo-flexural nano-positioning stages," *IEEE/ASME Transactions on Mechatronics*, vol. 14, pp. 11-20, 2009.
- [15] C. Y. Su, Y. Stepanenko, J. Svoboda, and T. P. Leung, "Robust adaptive control of a class of nonlinear systems with unknown backlash-like hysteresis," *IEEE Transactions on Automatic Control*, vol. 45, pp. 2427-2432, 2000.
- [16] H. Aderiaens, W. Koning, and R. Baniq, "Modeling piezoelectric actuators," *IEEE/ASME Transactions on Mechatronics*, vol. 5, pp. 331-341, 2000.
- [17] Smith R., *Smart material systems: Model developments*, SIAM, Philadelphia, PA.